



# CHORUS

This is the accepted manuscript made available via CHORUS. The article has been published as:

## Low-spin states in $^{86}\text{Kr}$ from the $(n,n')$ reaction

N. Fotiades, M. Devlin, R. O. Nelson, and T. Granier

Phys. Rev. C **87**, 044336 — Published 29 April 2013

DOI: [10.1103/PhysRevC.87.044336](https://doi.org/10.1103/PhysRevC.87.044336)

# Low-spin states in $^{86}\text{Kr}$ from the $(n, n')$ reaction.

N. Fotiades,\* M. Devlin, and R. O. Nelson

*Los Alamos National Laboratory, Los Alamos, New Mexico 87545, USA*

T. Granier

*CEA, DAM, DIF, F-91297 Arpajon, France*

(Dated: March 28, 2013)

## Abstract

**Background:**  $^{86}\text{Kr}_{50}$  is a neutron-rich nucleus amenable to shell model calculations due to the shell closure at  $N = 50$ . It is also produced as a fragment in the fissioning of actinides. **Purpose:** The level structure of  $^{86}\text{Kr}$  at low excitation energies needs additional investigation for detailed comparison with calculations from theoretical models. By determining the cross sections for transitions that feed directly the ground state of  $^{86}\text{Kr}$  a large fraction of the total cross section for the  $^{86}\text{Kr}(n, n')^{86}\text{Kr}$  reaction channel can be obtained. **Methods:** Low-spin states of  $^{86}\text{Kr}$  were populated in the  $^{86}\text{Kr}(n, n'\gamma)$  reaction and were studied with the GEANIE Ge-detector array. The broad-spectrum pulsed neutron beam of the Los Alamos Neutron Science Center's (LANSCE) WNR facility provided neutrons in the energy range from 1 to above 600 MeV. The time-of-flight technique was used to determine the incident-neutron energies. **Results:** Partial  $\gamma$ -ray cross sections were measured for 21  $\gamma$ -rays of  $^{86}\text{Kr}$  and for neutron energies  $1 \text{ MeV} < E_n < 20 \text{ MeV}$ . A large part of the total cross section for the  $^{86}\text{Kr}(n, n')^{86}\text{Kr}$  reaction is observed. Ten transitions are observed for the first time and are placed on the level scheme at excitation energies below 3.7 MeV doubling the number of placed transitions up to this excitation energy. These transitions deexcite five previously known levels, among them the second and third  $0^+$  states, and one new level. The excitation energy of these levels was more accurately determined and the relative intensities of their decay paths were measured. All previously known levels up to 3.7 MeV excitation energy were identified, and the new level was added at 2917-keV excitation energy. Predictions from shell model calculations are compared with the data.

PACS numbers: PACS number(s): 23.20.Lv, 25.40.Fq, 27.50.+e, 28.20.-v

---

\* fotia@lanl.gov

## I. INTRODUCTION

$^{86}\text{Kr}$  is a neutron-rich nucleus and is also the heaviest stable Kr isotope.  $^{86}\text{Kr}$  features a closed neutron shell at  $N = 50$  and is the lightest stable  $N = 50$  nucleus. Hence, shell model calculations have been performed often for this nucleus [1–5] since it is amenable to such calculations. Comparison of these predictions with experimental results is essential to test the validity and improve on such calculations. The existing information on the low-spin structure of  $^{86}\text{Kr}$  is summarized in Ref. [6] and has been obtained mostly from  $\beta$ -decay measurements [7, 8], pickup reactions [9, 10] and proton scattering reactions [11]. Information on the higher-spin structure of  $^{86}\text{Kr}$  is also available [3, 6, 12].

It is interesting to further study the structure of  $^{86}\text{Kr}$  via a neutron-induced reaction. Such a study has never been reported [6] before the present work. Since  $^{86}\text{Kr}$  is stable, the  $(n, n')$  reaction can be used to investigate states in this nucleus. This reaction tends to be very non-selective and populates the majority of off-yrast low-spin and low-excitation-energy states [13–15]. Due to the non-selective mode of the reaction used here all previously known levels [6] with excitation energy up to 3.7 MeV were observed, the excitation energies of some levels were more accurately determined, and one level at 2917-keV excitation energy was added in the present work.

Reactions of fast neutrons on fission fragments are of increasing interest in the understanding of neutron-rich environments [16].  $^{86}\text{Kr}$  is such a fragment. Since the majority of fission fragments are unstable, the cross sections used for such interactions are necessarily the result of calculations using models most often based on measured data from reactions on stable nuclei. While there exists a considerable amount of such data, in many cases it is often incomplete in that the data are concentrated at neutron energies near 14 MeV, and because many neutron-rich stable nuclei are not well-studied. By determining the absolute cross sections for transitions that directly feed the ground state of  $^{86}\text{Kr}$  in the present work a large fraction of the total cross section for the  $^{86}\text{Kr}(n, n')^{86}\text{Kr}$  reaction channel can be obtained. This, coupled to a theoretical calculation, will give confidence or suggest improvement in the reaction models as they are extended to heavier, unstable Kr isotopes.

## II. EXPERIMENT

The discrete  $\gamma$  rays of  $^{86}\text{Kr}$  were detected using the Ge  $\gamma$ -ray spectrometer GEANIE [17, 18] as a function of incident neutron energy. The neutrons were provided by the “white” source neutron beam at the LANSCE/WNR facility [19, 20]. GEANIE is located 20.34 m from the WNR spallation neutron source on the 60°-Right flight path. During the experiment GEANIE was comprised of 10 Compton-suppressed planar Ge detectors (Low Energy Photon Spectrometers - LEPS) and 10 Compton-suppressed coaxial Ge detectors. The planar detectors have very low detection efficiency for  $\gamma$  rays with energies above  $\sim 0.9$  MeV. Since most of the excited states observed produce  $\gamma$  rays with energies greater than 1 MeV, the results presented here come from the coaxial detectors only, and in particular from four coaxial detectors that were selected for the best energy and time resolution. The neutrons are produced in a  $^{nat}\text{W}$  spallation target driven by an 800 MeV proton beam with an average current of  $\sim 2$   $\mu\text{A}$ . The beam time structure was as follows: 40 Hz of “macropulses”, 625  $\mu\text{s}$  long, each macropulse containing approximately 340 “micropulses”, spaced every 1.8  $\mu\text{s}$ . The energy of the neutrons was determined using the time-of-flight (TOF) technique. The neutron flux on target was measured with a fission chamber, consisting of  $^{235}\text{U}$  and  $^{238}\text{U}$  foils [21], located on the same flight path, 18.48 m from the center of the spallation target.

The target cell containing the  $^{86}\text{Kr}$  isotopically enriched gas consisted of one cylinder, 6.261 cm long and with a radius of 1.7975 cm. The cylindrical horizontal walls were 0.525 mm thick and made of aluminum. The planar walls, orthogonal to the neutron beam, were very thin mylar foils. The pressure of the  $^{86}\text{Kr}$  gas inside the cell was  $\sim 450$  kPa. During two days of the experiment two natural Fe 5 cm circular foils, 0.05 mm thick, were placed in front and in the back of the  $^{86}\text{Kr}$  gas cell. The plane of the Fe foils was at an angle of  $90^\circ$  with respect to the beam. The Fe foils were included so that the known cross section at  $E_n = 14.5$  MeV [22] of the strong 846.8-keV,  $2^+ \rightarrow 0^+$  transition of  $^{56}\text{Fe}$ , produced in natural Fe from inelastic scattering, was used to normalize the cross sections obtained in the present experiment.

The time-resolution of the Ge detectors is the dominant factor that determines the incident neutron energy resolution. The time resolution varies as a function of incident  $\gamma$ -ray energy, and ranged from 10 to 20 ns (FWHM) for the coaxial Ge detectors. Corrections for the finite beam spot size,  $\gamma$ -ray attenuation in the target (both Kr and Fe), and the

contribution from neutrons produced by scattering and reactions in the targets (secondary effects), were modeled using the MCNPX Monte-Carlo radiation transport code [23]. Electronic “dead-times” were measured using scalers. A total of  $\sim 2.3 \times 10^8$   $\gamma$  singles and higher fold data were recorded in the coaxial detectors used in the analysis.

In the off-line analysis a matrix of  $\gamma$ -ray energy versus TOF was built for the coaxial detectors. By gating on the TOF axis  $\gamma$ -ray spectra corresponding to selected neutron energy bins are obtained. Fitting peaks in these spectra gives the yield of a  $\gamma$  ray for a certain neutron energy bin. The neutron flux versus neutron energy was deduced from the fission chamber. The absolute partial  $\gamma$ -ray cross sections can then readily be obtained (see, for instance, Ref. [18]). All cross sections obtained in the present work are normalized to the cross section at  $E_n = 14.5$  MeV [22] of the 846.8-keV,  $2^+ \rightarrow 0^+$  transition of  $^{56}\text{Fe}$ . The  $\gamma$ - $\gamma$  data obtained in the present work could not be used to establish coincidence relations between transitions due to insufficient statistics in the resulting gated spectra.

### III. EXPERIMENTAL RESULTS

The cross sections for emission of a total of 21  $\gamma$ -rays of  $^{86}\text{Kr}$  were determined. All transitions are included in the level scheme shown in Fig. 1 and summarized in Table I. Before the present work, for excitation energies up to 3.7 MeV, only nine transitions were known [6]. In the present work ten transitions were added in the level scheme up to 3.7 MeV excitation energy, thus more than doubling the transitions of  $^{86}\text{Kr}$  up to this excitation energy. These transitions are the 376.8-, 660.3-, 666.7-, 1162.0-, 1191.6-, 1352.1-, 1763.5-, 1976.9-, 2018.8-, and 3010-keV in Fig. 1 that are observed for the first time. The 1565-keV  $\gamma$ -ray peak in the spectra is an unresolved doublet from the 1564.8- and 1566.3-keV transitions of  $^{86}\text{Kr}$ , thus the number of transitions present in the level scheme is 22.

An example of the cross sections obtained in the present work for previously-known  $^{86}\text{Kr}$  transitions is shown in Fig. 2 and exhibit the characteristic of the  $(n, n')$  reaction channel, namely, they peak below 10 MeV incident-neutron energy where the  $(n, 2n)$  reaction channel opens up. The cross sections obtained for all new transitions assigned to  $^{86}\text{Kr}$  in the present work exhibit this characteristic, as for example, is shown in Fig. 3 for two of the ten new transitions observed in the present work. Moreover, as it can be seen in Figs. 2 and 3, the  $\gamma$ -ray cross sections in the  $(n, n')$  reaction channel decrease rapidly above 10 MeV,

hence the results presented here were focused on the incident-neutron energy range of 1-20 MeV, although the facility provides neutrons with energies up to several hundred MeV. The relative detector efficiencies used in obtaining all cross sections were determined using a  $^{152}\text{Eu}$  calibrated  $\gamma$ -ray source with the highest  $\gamma$  ray at 1408.0 keV. Above this  $\gamma$ -ray energy an extrapolation was used which is deemed reasonable up to at least 2926 keV  $\gamma$ -ray energy since it reproduced within uncertainties the previously reported  $\gamma$ -ray relative intensities for the transitions deexciting the 2349.78- and 2926.32-keV levels of  $^{86}\text{Kr}$  [6]. Specifically, for the 2350-keV level in Fig. 1 the intensity of the 785.2-keV transition is 45(3)% the intensity of the 2349.6-keV transition, and for the 2926-keV level the intensity of the 2926.1-keV transition was found to be 19(4)% the intensity of the 1361.7-keV transition. All cross-section uncertainties in this work are statistical. Estimated total systematic uncertainties of 10-18% (depending on  $E_\gamma$  and  $E_n$  energies) are additional and include 2-8% from detection efficiency (varies with  $E_\gamma$  and is larger for the energies where extrapolation was used), 1-3% from the neutron flux (varies with  $E_n$ ), as well as contributions from the target thickness and “dead-time” corrections that do not depend on  $E_\gamma$  and  $E_n$ .

In  $^{86}\text{Kr}$  three excited  $0^+$  states have been observed [6] at excitation energies 2724(4)-, 3540(5)-, and 3832(10)-keV, but no transitions were previously reported to deexcite these states. In the present work two transitions were observed to deexcite each of the 2724(4)- and 3540(5)-keV states of  $^{86}\text{Kr}$ , and their excitation energy is now much more accurately determined as 2726.8(7)- and 3541.7(8)-keV, respectively (see Fig. 1). Moreover, three previously known states at excitation energies 3010(6)-, 3325(8)-, and 3575(10)-keV [6], for which no deexciting transitions were observed before, were also accurately determined in the present work at 3010.1(6)-, 3328.3(9)- and 3583.5(9)-keV, respectively, through observation of transitions from these states to lower levels. Finally, a new state was placed in the level scheme at excitation energy 2916.7(8)-keV and deexcites via two transitions to the lower  $2_1^+$  and  $4_1^+$  states. In all cases the assignment of two transitions as deexciting the same state is based on the observed very similar excitation functions for the two transitions, as seen in Fig. 3 where the excitation functions of the two transitions deexciting the 3010-keV level are very similar and in Fig. 4 where the cross sections obtained for the rest of the new transitions are shown.

The four coaxial detectors used in the analysis in the present experiment were at angles  $-51^\circ$ ,  $-77^\circ$ ,  $78.5^\circ$ , and  $102^\circ$  with respect to the neutron beam. The effect of angular distribu-

tions of the  $\gamma$  rays was considered using the AVALANCHE code [24] to model the feeding of the excited states of  $^{86}\text{Kr}$ . The angular distribution correction factors were obtained as described in Refs. [18, 25]. All transitions shown in Fig. 2 were corrected for this effect assuming a stretched  $E2$  multipolarity. For the doublet 1565-keV transition in Fig. 2 a 10% contribution from an  $M1/E2$  1566.3-keV transition was assumed in the calculation of the angular distribution correction factor. An angular distribution correction is not needed for the transitions emitted by the  $0^+$  states in Fig. 1 since the  $\gamma$ -ray distribution in the  $(n, n')$  reaction is isotropic when the spin of the initial state is zero. No correction was applied to the rest of the transitions in Figs. 3 and 4 because of the uncertainty in the spin and/or parity of the initial states and in the multipolarity of the emitted transitions. The angular distribution correction was less than 1% for incident-neutron energies above 5 MeV and the maximum correction was 18% for the 685.3 keV transition in Fig. 1 at incident-neutron energies right above the threshold of population of the 2250-keV initial level.

#### IV. DISCUSSION

The level at 3010-keV was assigned a spin-parity  $(1-5)^+$  in the latest evaluation [6]. The decay out of this level established in the present work narrows this down to  $(1,2)^+$ . This level was previously observed in  $(t, \alpha)$  [9] and  $(p, p')$  [11] reactions. This level was reported to have a significant  $l = 3$  spectroscopic factor in the proton pick-up reaction and a  $(1,2)^+$  assignment was originally suggested [9], in agreement with the result of the present work. A relative intensity between the two decay paths of the 3010-keV level was obtained from the present data and the 660.3-keV transition was found to carry 75(6)% the intensity of the 3010-keV transition. The new level observed at 2916.7-keV excitation energy can be assigned a  $(2^+, 3, 4^+)$  spin-parity based on the established decay paths. This level is new in the sense that it is not included in the latest evaluation [6]. However, a 2917(6)-keV level was first reported in the  $(t, \alpha)$  [9] reaction with a  $(3, 4)^+$  spin-parity assignment. Due to the large error in the excitation energy of the 2917(6)-keV level, most likely this level in the evaluation was identified as identical to the 2926-keV level observed in  $\beta$ -decay [7, 8] and  $(p, p')$  reactions [11]. In the present work, the combination of level population through a reaction that is non-selective with the high energy resolution of the GEANIE array allowed the observation of clearly distinguishable decay paths out of both levels suggesting that the

2916.7-keV state is a separate level and a  $(3,4)^+$  spin-parity can be assigned to it based on the present work and the results from Ref. [9]. For the transitions in Fig. 1 that deexcite the 2917-keV level, the intensity of the 1352.1-keV transition was determined to be 25(4)% relative to the intensity of the 666.7-keV transition. The intensity of the 376.8-keV transition, deexciting the first excited  $0^+$  state, is 70(6)% relative to the intensity of the 1162.0-keV transition, and the intensity of the 1976.9-keV transition, deexciting the second excited  $0^+$  state, is 50(8)% relative to the intensity of the 1191.6-keV transition.

$^{86}\text{Kr}$  has eight more protons than the doubly magic  $^{78}\text{Ni}$ . The heavier-than- $^{78}\text{Ni}$   $N = 50$  isotones are a good test ground for possible existence of collectivity close to  $^{78}\text{Ni}$  and of the rigidity of the  $N = 50$  shell closure. Generally, semi-magic nuclei, like  $^{86}\text{Kr}$ , are expected to have a near-spherical shape due to the neutron or proton shell closure. Indeed, the level structures at low excitation energies for the lighter even-mass  $N = 50$  isotones  $^{82}\text{Ge}$  [26],  $^{84}\text{Se}$  [27], and, to a lesser extent for  $^{86}\text{Kr}$ , show some resemblance to that of a vibrator exhibiting a clustering of the  $0_2^+$ ,  $2_2^+$  and  $4_1^+$  states. However, two-particle two-hole (2p-2h) excitations coupled to  $0^+$  can drive the nucleus to a larger deformation even at low excitation energies. The first two  $0^+$  excited states, for which the 2726.8(7)- and 3541.7(8)-keV excitation energies were established in the present work, were recently interpreted as 2p-2h excited states associated with two different open-shells of  $Z=28-50$  and  $28-40$  [28]. Similar cases were also identified in the  $N = 50$  isotones  $^{82}\text{Ge}$  and  $^{84}\text{Se}$  [28]. The previously known 4111(10)-keV,  $2^+$  level of  $^{86}\text{Kr}$  [6] is suggested in Ref. [28] as being the first excited state of the deformed rotational band built on the  $0^+$  state at 3542-keV excitation energy. No new transition was observed in the present work that could match the pattern of deexcitation expected for such a level, hence, such transition(s) lie below the detection limit of the present experiment. Similarly, no candidate state was observed in the present experiment for the  $2^+$  level of the deformed rotational band built on the  $0^+$  state at 2727-keV excitation energy.

Shell model calculations for  $^{86}\text{Kr}$  [1–5] have been used to further investigate the underlying nuclear structure in this nucleus. The more extensive calculations are those described in Refs. [4, 5]. In both calculations the 3010-keV state is assumed to be the  $1_1^+$  level that the shell model predicts at excitation energies near the experimental result. Also, both calculations assume that the 2926-keV level is the  $3_1^+$  level predicted by the shell model. However, the  $3_1^+$  level is, most likely, the 2917-keV level established in the present work, and the 2926-keV level is, thus, the  $2_3^+$  level predicted also by both calculations (see Fig. 5).



Most of the feeding of the ground state of  $^{86}\text{Kr}$  in the  $(n, n')$  reaction is expected to flow through the 1564.8-keV transition that deexcites the first  $2^+$  state. Indeed, almost all decaying  $\gamma$  cascades proceed through the  $2_1^+ \rightarrow 0_1^+$  transition as has been noted previously at lower reaction energies [29–31]. Under the implicit assumption that the direct population of the ground state via  $(n, n')$  (i.e., without any  $\gamma$  emission) is negligible, the cross section obtained for the 1564.8-keV transition represents a large fraction of the total cross section for the  $^{86}\text{Kr}(n, n')^{86}\text{Kr}$  reaction channel. However, the 1564.8- and 1566.3-keV transitions of  $^{86}\text{Kr}$  form a doublet in our data and the contribution of the latter to the total can not be eliminated. The apparent small jumps in the partial cross section for the 1565-keV line in Fig. 2 for  $E_n \sim 5$  MeV could be due to the 1566.3-keV line indicating that the 3816-keV level is most likely populated in the present reaction. However, assuming that the 1566.3-keV transition has a similar strength to the 1814.1- (see Fig. 2) and 1685.1-keV transitions of  $^{86}\text{Kr}$  in Fig. 1 then the strength of the 1566.3-keV transition represents less than  $\sim 10\%$  of the total 1565-keV strength plotted in Fig. 2. Hence, the cross section of the 1565-keV transition plotted in Fig. 2 should be a good estimate of the total cross section for the  $^{86}\text{Kr}(n, n')^{86}\text{Kr}$  reaction channel, assuming at least a 10% uncertainty. This is the first experimental determination of the  $^{86}\text{Kr}(n, n')^{86}\text{Kr}$  reaction cross section and should aid in benchmarking theoretical calculations that predict  $(n, xn)$  cross sections on neutron-rich nuclei.

## V. SUMMARY

In conclusion, partial cross sections for 21 transitions in the  $^{86}\text{Kr}(n, n'\gamma)$  reaction channel have been measured for neutron energies  $1 \text{ MeV} < E_n < 20 \text{ MeV}$ . Ten of these transitions were observed for the first time and were assigned to  $^{86}\text{Kr}$  based on the determination of their cross sections versus incident-neutron energies. These transitions were added in the level scheme up to 3.7 MeV excitation energy, thus doubling the transitions assigned to  $^{86}\text{Kr}$  up to this excitation energy. Eight of these transitions deexcite five previously known levels, among them the second and third  $0^+$  states, while two transitions were observed to deexcite one new level. A large fraction of the total cross section for the  $^{86}\text{Kr}(n, n')^{86}\text{Kr}$  reaction has now been observed.

## ACKNOWLEDGMENTS

This work was performed under the auspices of the U.S. Department of Energy (DOE) under Contract No. DE-AC52-06NA25396 and of an agreement between CEA/DAM and NNSA/DP on cooperation on fundamental science. This work has benefitted from use of the LANSCE accelerator facility supported under DOE Contract No. DE-AC52-06NA25396. The authors thank Dr. Thierry Ethvignot for providing the  $^{86}\text{Kr}$  gas sample.

- 
- [1] D. Verney *et al.*, Phys. Rev. C **76**, 054312 (2007).
- [2] K. Kaneko, M. Hasegawa, T. Mizusaki, and Y. Sun, Phys. Rev. C **74**, 024321 (2006).
- [3] G. Winter *et al.*, Phys. Rev. C **48**, 1010 (1993).
- [4] J. Sinatkas, L. D. Skouras, D. Strottman, and J. D. Vergados, J. Phys. G **18**, 1377 (1992).
- [5] X. Ji and B. H. Wildenthal, Phys. Rev. C **40**, 389 (1989).
- [6] B. Singh, Nucl. Data Sheets **94**, 1 (2001).
- [7] E. Achterberg *et al.*, Phys. Rev. C **5**, 1587 (1972).
- [8] M. H. Hurdus and L. Tomlinson, J. Inorg. Nucl. Chem. **37**, 1 (1975).
- [9] A. B. Tucker, K. E. Apt, J. D. Knight, and C. J. Orth, Phys. Rev. C **6**, 2075 (1972).
- [10] E. R. Flynn, J. D. Sherman, N. Stein, D. K. Olsen, and P. J. Riley, Phys. Rev. C **13**, 568 (1976).
- [11] B. K. Arora, D. K. Olsen, P. J. Riley, and C. P. Browne, Phys. Rev. C **10**, 2301 (1974).
- [12] A. Prévost *et al.*, Eur. Phys. J. A **22**, 391 (2004).
- [13] T. Belgya, R. A. Gatenby, E. M. Baum, E. L. Johnson, D. P. DiPrete, S. W. Yates, B. Fazekas, and G. Molnár, Phys. Rev. C **52**, R2314 (1995).
- [14] S. W. Yates, J. Phys. G: Nucl. Part. Phys. **31** S1393 (2005).
- [15] N. Fotiades, R. O. Nelson, and M. Devlin, Phys. Rev. C **81**, 037304 (2010).
- [16] T. Watanabe, T. Kawano, M. B. Chadwick, R. O. Nelson, S. Hilaire, E. Bauge, and P. Dossantos-Uzarralde, J. Nucl. Sci. Technol. **47**, 470 (2010).
- [17] J. A. Becker and R. O. Nelson, Nuclear Physics News International **7**, 11 (June, 1997)
- [18] N. Fotiades *et al.*, Phys. Rev. C **69**, 024601 (2004).
- [19] P. W. Lisowski, C. D. Bowman, G. J. Russell, and S. A. Wender, Nucl. Sci. Eng. **106**, 208 (1990).
- [20] P. W. Lisowski and K. F. Schoenberg, Nucl. Instr. Meth. in Phys. Res. A **562**, 910 (2006).
- [21] S. A. Wender, S. Balestrini, A. Brown, R. C. Haight, C. M. Laymon, T. M. Lee, P. W. Lisowski, W. McCorkle, R. O. Nelson, and W. Parker, Nucl. Instr. Meth. A **336**, 226 (1993).
- [22] R. O. Nelson, N. Fotiades, M. Devlin, J. A. Becker, P. E. Garrett, and W. Younes, Proceedings of the International Conference on Nuclear Data for Science and Technology, Santa Fe, New Mexico, 2004, ed. R. Haight, M. B. Chadwick, T. Kawano and P. Talou, AIP Conference

- Proceedings 769, 838 (2005).
- [23] MCNPX User's Manual, Version 2.6.0, edited by D. B. Pelowitz, Los Alamos National Laboratory Controlled Publication LA-CP-07-1473 (2007)
  - [24] P. Cejnar, S. Drissi, and J. Kern, Nucl. Phys. A **602** 225 (1996).
  - [25] S. MacMullin *et al.*, Phys. Rev. **C 85**, 064614 (2012).
  - [26] J. K. Tuli, Nucl. Data Sheets **98**, 209 (2003).
  - [27] D. Abriola *et al.*, Nucl. Data Sheets **110**, 2815 (2009).
  - [28] J. K. Hwang, J. H. Hamilton and A. V. Ramayya, Int. J. Mod. Phys., Vol. 21, No. 3, 1250020 (2012).
  - [29] R. B. Day, Phys. Rev. **102**, 767 (1956).
  - [30] J. R. Huizenga and R. Vandenbosch, Phys. Rev. **120**, 1305 (1960).
  - [31] R. Vandenbosch and J. R. Huizenga, Phys. Rev. **120**, 1313 (1960).

TABLE I. Level excitation energy, spin and parity and  $\gamma$ -ray energy and intensity, for all levels and transitions in Fig. 1. Transitions indicated by an asterisk are observed for the first time.

$E_x$ (keV)	$J^\pi$	$E_\gamma$ (keV)	$I_\gamma$
1565	$2^+$	1564.8	100
2250	$4^+$	685.3	100
2350	$2^+$	785.2	45(3)
		2349.6	100
2727	$0^+$	376.8*	70(6)
		1162.0*	100
2850	$(2,3)^+$	500.4	16(11)
		1285.9	100(10)
2917	$(3,4)^+$	666.7*	100
		1352.1*	25(4)
2926	$(2)^+$	1361.7	100
		2926.1	19(4)
3010	$(1,2)^+$	660.3*	75(6)
		3010*	100
3099	$3^-$	1534.7	100
3328	$(^+)$	1763.5*	100
3542	$0^+$	1191.6*	100
		1976.9*	50(8)
3584		2018.8*	100
3816	$(5^+,6^+)$	1566.3	100
3935	$(5)$	1685.1	100
4064	$(6^+)$	1814.1	100

FIG. 1. Level scheme showing the transitions of  $^{86}\text{Kr}$  observed in the present work. All  $\gamma$ -ray and level energies are in keV.

FIG. 2. Cross sections for the 1565-, 685-, and 1814-keV transitions of  $^{86}\text{Kr}$ . The first is a doublet including the 1564.8- and 1566.3-keV transitions in Fig. 1 and is the strongest transition observed in the present work.

FIG. 3. Cross sections for the 660.3- and 3010-keV transitions of  $^{86}\text{Kr}$  deexciting the 3010-keV level in Fig. 1.

FIG. 4. Cross sections for transitions of  $^{86}\text{Kr}$  deexciting the (a) 2727-, (b) 3542-, (c) 2917-, (d) 3328- and 3584-keV levels Fig. 1.

FIG. 5. Comparison of  $^{86}\text{Kr}$  levels as established experimentally in the present work to previous shell-model predictions [4, 5].

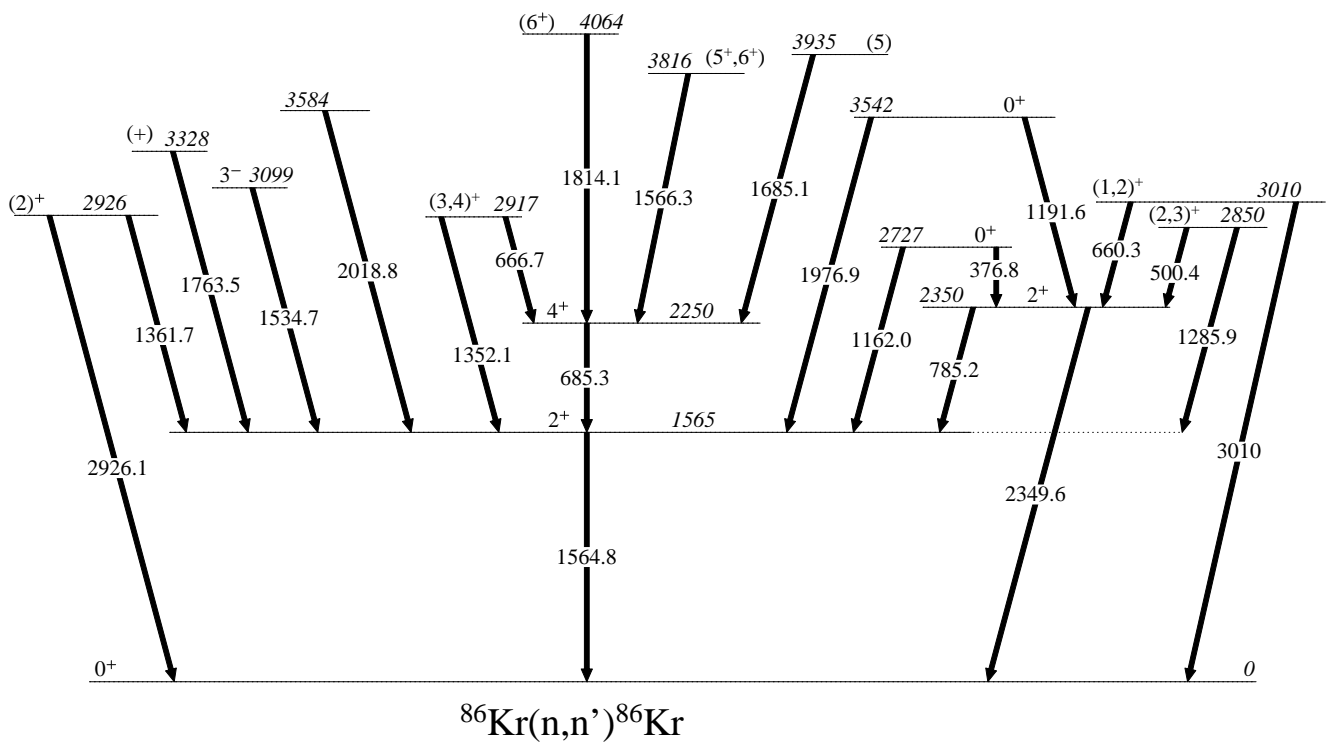


Figure 1

CB10336

28Mar2013

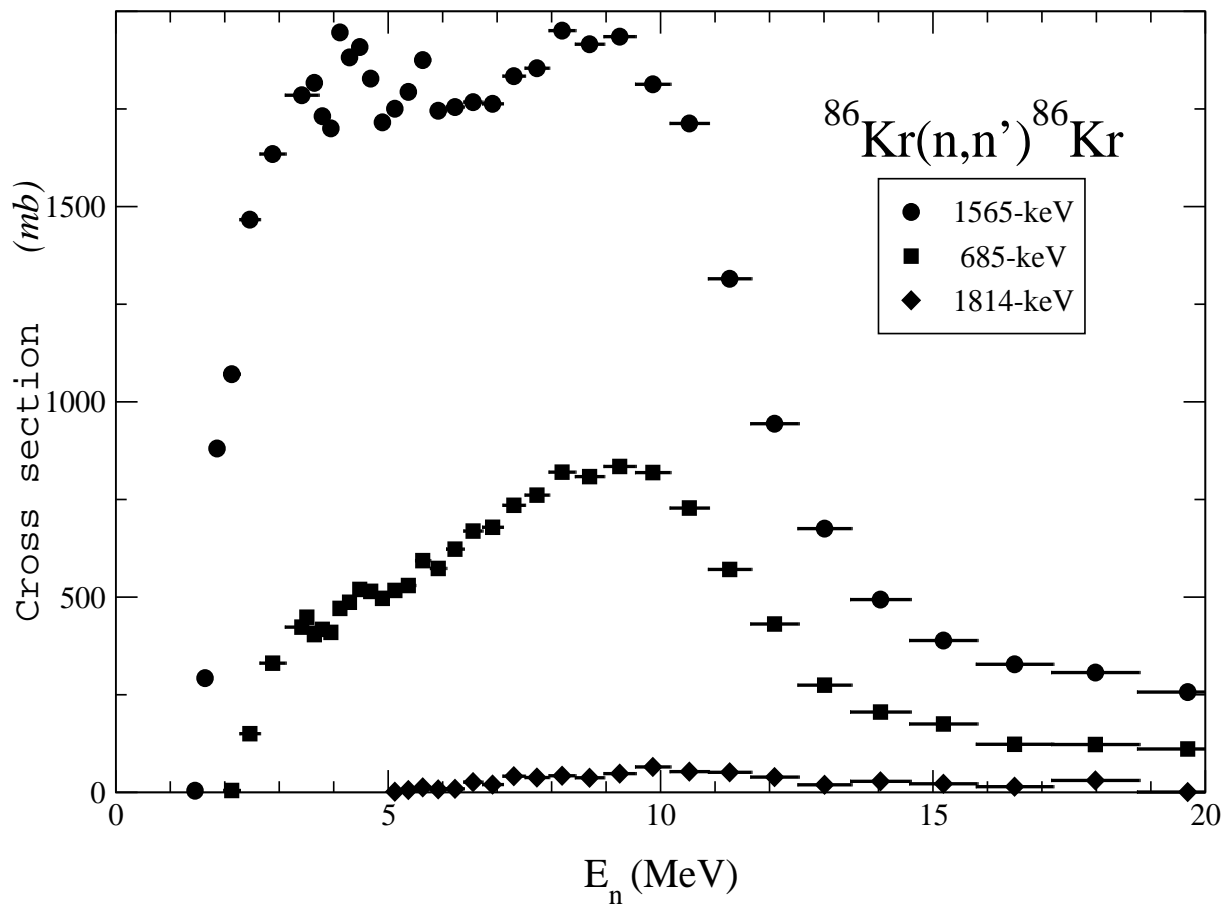


Figure 2

CB10336

28Mar2013



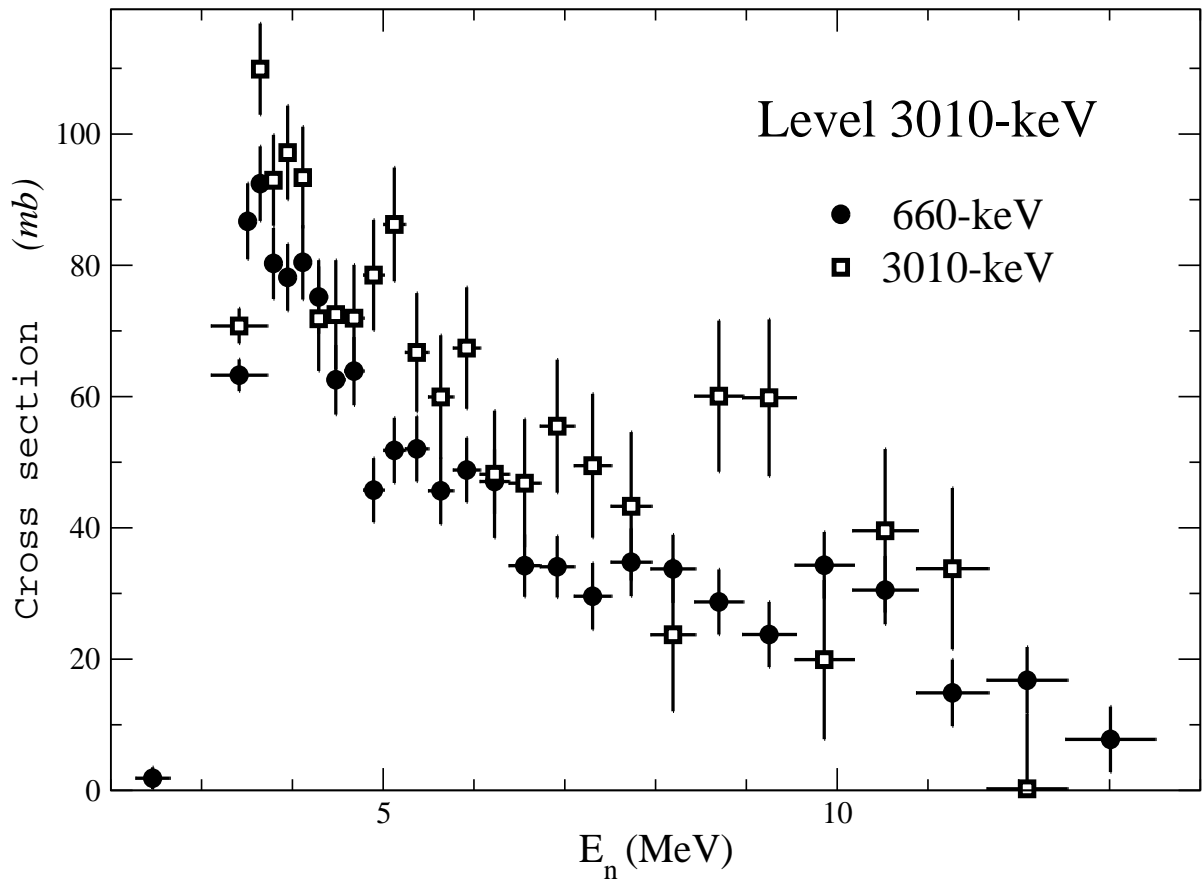


Figure 3

CB10336

28Mar2013

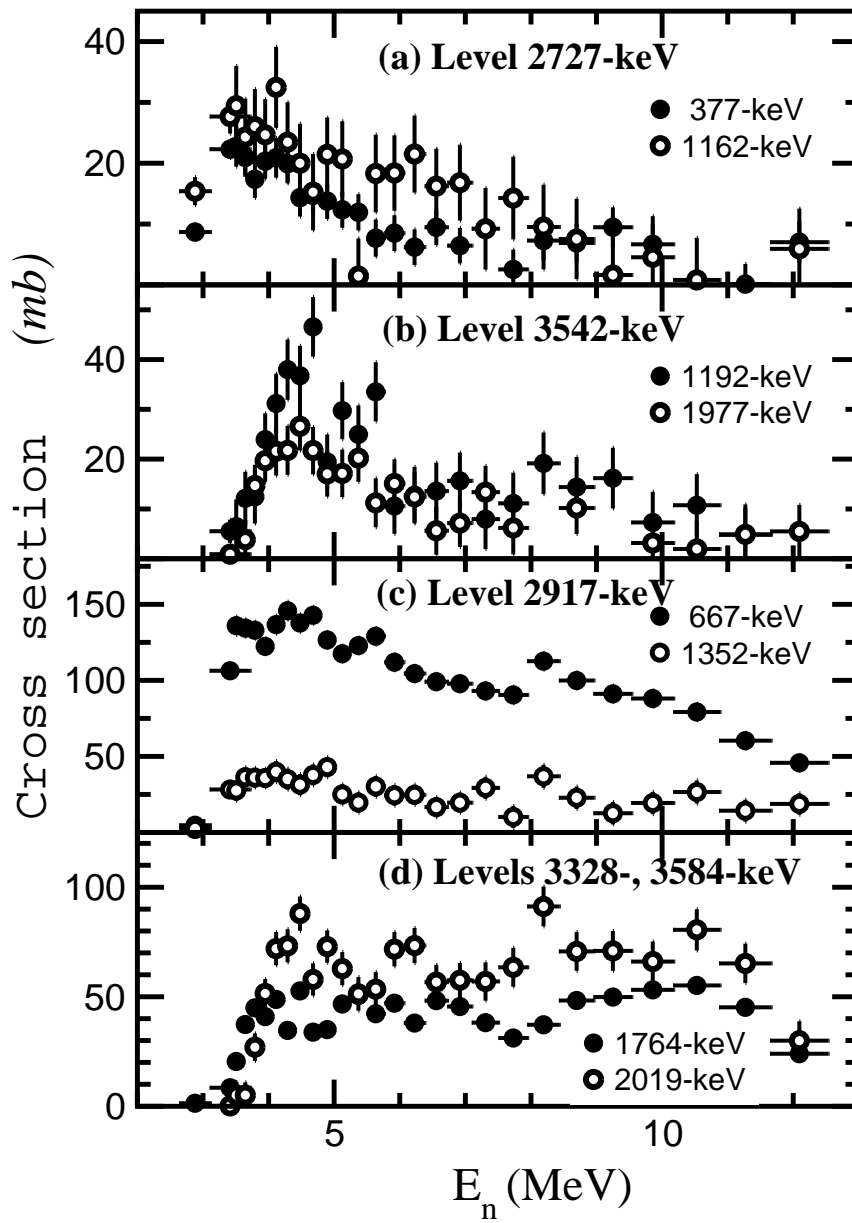


Figure 4

CB10336

28Mar2013

